Fabrication of Metal Nanospheres and the Kinetics Controlled with High-Flux Negative Ions and the Optical Properties

N. Kishimoto, V.T. Gritsyna*, Y. Takeda and C.G.Lee

National Research Institute for Metals, 1-2-1 Sengen, Tsukuba, Ibaraki 305, Japan
** Kharkov State University, Kharkov 310077, Ukraine*

(Received: 17 February 1998; accepted: 26 March 1998)

Abstract

Nanoparticles of Cu were fabricated with negative-ion implantation at high beam fluxes. Focusing on kinetic aspects, we studied the dose-rate dependence of nanoparticle formation and resultant optical properties. Negative-Cu ions of 60 keV were implanted into silica glasses up to 260 μA/cm², fixing the total dose at 3.0×10^{16} ions/cm². Spherical Cu nanocrystals spontaneously formed within a narrow region, near the projectile range of Cu ions. Small dots coexisted in a region deeper than the projectile range. Optical properties were significantly dependent on both the dose rate and the specimen boundary condition. Beam-surface interactions affect Cu- retention in the substrate. The nanoparticle growth is controlled by surface tension and radiation-induced diffusion. Nanoparticles may be self-organized under a balance between the exterior and the interior processes.

1. Introduction

Metal nanoparticles, embedded in dielectrics, have recently attracted attention for developing nonlinear electronic and optical properties [1], enhanced by surface plasmon resonance[2]. Various fabrication methods, from conventional thermal precipitation to state-of-the-art atom manipulation, have been applied for nanoparticle fabrication. The variety of nanoparticle systems is expanding, not only to widen materials selection (including chemical compounds or alloys) but also to control the morphology. In order to attain a desirable nanoparticle system for optical devices, a fabrication method requires spatial controllability, i.e., particle size, density or positioning, to be free of defects and availability of a mass, expecially for optical applications.

Figure 1 shows a schematic chart of various available methods, in respect to atomistic controllability, nonequilibrium nature and mass availability. Each method has different degrees of merit, but few methods simultaneously meet a desired spatial controllability and freedom from defects. Increasing non-equilibrium artificiality causes a loss of natural mechanisms to accommodate atomic defects, and *vice versa*. Among those methods, we have employed ion implantation emphasizing spatial controllability. In particular, we have aimed at a nanoparticle system, distributed within a narrow thickness, i.e., a *two dimensional* distribution. Such a nanostructure may become important for future device applications. However, surface charging with

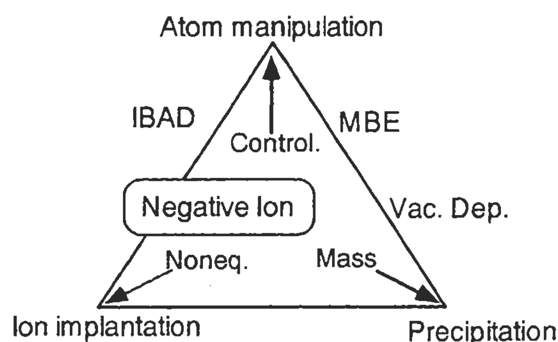

Fig.1 Schematic diagram of characteristics in various fabrication methods, in comparison with low-energy negative ion implantation.

positive ions may be fatal impeding low-energy implantation [3]. From this aspect, negative-ion implantation of a low energy is one of the most promising methods, balancing with secondary electron emission. As seen in Fig. 1, the present method falls on an intermediate position, which has fair controllability and non-equilibrium characteristics. Furthermore, high-current implantation may compensate for the defect production inherent in ion bombardment. In this paper, we discuss material kinetics at high dose rates and explore a possibility to control the nanoparticle formation, optimizing the dose rate.

2. Experimantal

Negative Cu ions of 60 keV were produced by a plasma-sputter-type ion source, as illustrated in Fig. 2. The ion source provided us with a well-oriented and intense negative beam, by virtue of special features, i.e., cusp

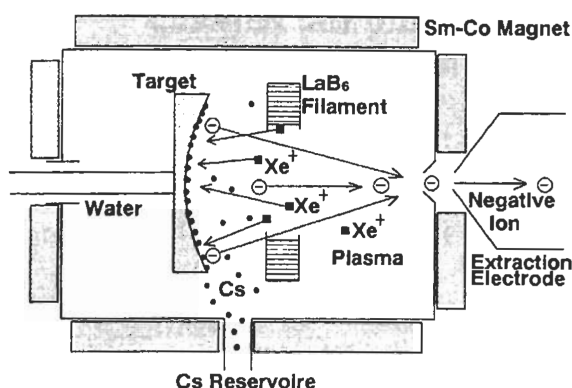

Fig.2 Negative heavy-ion source of plasma-sputter type with multi-cusp magnetic fields.

magnetic fields, Xe-sputtering and Cs supply [4]. A total Cu- current of 3 - 4 mA was attained at the specimen position, after a mass analyzing magnet through a triplet-quadrupole lens. The energy and charged state of the negative ions are well-defined and free from charge-neutralization effects, in contrast to other ionized deposition methods. The dose rate ranged up to 260 $\mu A/cm^2$, fixing a total dose of 3.0×10^{16} $ions/cm^2$. The maximum dose rate corresponds to a deposition rate of 0.2 nm/s for pure Cu and is comparable with that of typical vapor deposition methods.

Depth profiles and sputtering yields for 60 keV Cu were roughly estimated with the TRIM code[5]. The projectile range and the straggling width obtained were 45 nm and 30 nm, respectively. The Cu concentration at the projectile peak corresponds to about 10 at. % of the substrate atoms, for the total dose.

Special care was taken of the specimen geometry and boundary conditions, which affected thermal and electromagnetic interactions between the beam and the surface. Substrates used were optical-grade silica glasses (KU-1: 820 ppm OH^-) of 15 mm diameter and 0.5 mm thick. A metal (Cu) mask, having 2 mm ϕ -holes (2.2 mm ϕ $\times 37$ holes) or a 12 mm ϕ hole, was mounted on the surface to determine the beam load. The Cu beam reached the substrate surface through the aperture hole(s).

Optical absorption and reflection were measured in a photon energy range from 1.4 to 6.5 eV using a dual beam spectrometer. Nonlinear optical susceptibility of the specimens was evaluated with a degenerate-four-wave mixing (DFWM) method.

Cross-sectional electron microscopy (TEM) was conducted to evaluate microstructures in the Cu-implanted region. After the ion implantation, a thin Cr film (5 nm) was deposited as a marker layer onto the implanted surface. Thickness of the cross-section was measured with a tilting method for the Cr layer.

3. Results and Discussion

In fabricating a nanostructure, i.e., two dimensionally-distributed nanoparticles, important requirements are to control 1) depth profile of implants, 2) roundness and diameter of particles, 3) number density of particles, etc. In principle, incident-ion energy uniquely determines the depth profile, and ion dose gives the total amount of particles, as far as the precipitation saturates. In order to control 2) and 3), a conventional approach is thermal annealing after implantation. Unless the precipitation completely saturates to the equilibrium state, thermal annealing is eligible for the morphology control. There is, however, a considerable risk of reducing the spatial controllability, if one applies the post-irradiation annealing. Therefore, we have focused on in-situ energy deposition from ions and its relaxation processes. The key parameter of ion implantation is *dose rate*, under a given total dose. Change in dose-rate may influence kinetics of the precipitation, via changes in either nucleation probability or growth rate. The in-beam processing may provide an optimum condition and be more effective than the post-irradiation treatment.

In-beam processes, in general, have been believed to be highly dynamical and dependent on dose rate. Magruder III et al [6] demonstrated occurrence of a great dose-rate-dependence on optical absorption, using positive Cu ions of 160 keV. On the other hand, there is an idea that equilibrium thermodynamics is almost valid, analogously with a high-temperature equilibrium attained by ion-beam heating. For instance, the diameter of particles seemed to be determined by the total amount of implants, irrespective of dose rate[7]. Consequently, it is necessary to analyze implications of the dose-rate dependence, when we apply this method to nanostructure control.

Fig. 3 shows a typical cross-sectional TEM-image of a silica glass, where 60 keV-Cu^- ions are implanted at a current density of 95 $\mu A/cm^2$, up to 3×10^{16} $ions/cm^2$. There are several features characteristic in the present ion implantation: Spherical Cu nanocrystals, of

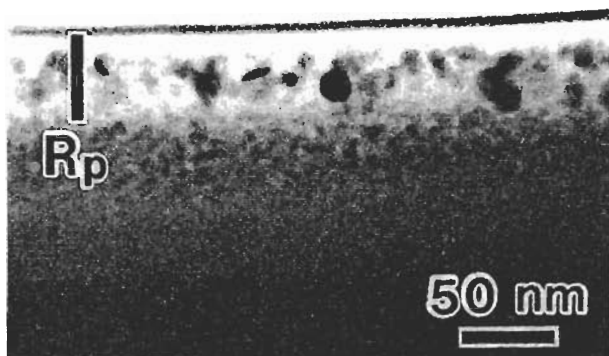

Fig.3 Cross-sectional TEM image of a specimen, 60 keV Cu^--implanted at 95 μA/cm², up to 3 x 10^{16} ions/cm². The R_P denotes a projectile range of the Cu ions.

15-20 nm in diameter, spontaneously form without post-irradiation annealing. Between the nanospheres, there are few discernible extended defects. Average position of the nanospheres is around the projectile range of 60 keV Cu ions, R_P=45 nm, but somewhat shallower than the R_P. The nanospheres are located in a range which is 2-3 times as much as the diameter. These features are basically consistent with predictions of 60 keV-Cu implantation, though precipitation is dominant. Pronounced roundness of the nanoparticles, such as droplets, is a significant merit for using high current density. It should be noted that the high current implantation was accomplished by negative ions, and also by use of the 2 mm ϕ - mask.

Other notable features in Fig. 3 are the fine copious particles of a few nm ϕ, which are distributed in the region deeper than R_P. The total range of Cu particles, including the deeper region, reaches 1.5 times as much as the TRIM prediction (~R_P + ΔR_P). Statistical analysis of Cu precipitates[8] indicated that a Cu-depleted region existed between the larger nanospheres and the deeper region. Consequently, the morphology of the Cu nanospheres above 10 nm ϕ shows a distinct bimodal distribution, both for size and depth distribution.

A mechanism of the nanosphere formation is explained by a droplet-model based on surface tension and radiation-enhanced diffusion, which increasingly become dominant at the higher dose rates. On the analogy with the droplet growth, a pressure balance with the surface tension gives a condition at the interface of the sphere with radius r,

$$P_S = P_M + \frac{2\gamma}{r}, \tag{1}$$

where P_S and P_M denote equilibrium pressures inside the sphere and the matrix, respectively, and γ is the surface energy. Driving force of the droplet growth is given by a concentration gradient resulting from a difference in equilibrium solute concentration, $C(r)$,

$$C(r) = C_\infty exp\frac{2V_S\gamma}{rk_BT}, \tag{2}$$

where C_∞ and V_S are the saturated concentration and the specific volume of atoms in the sphere, respectively. Since solute concentration surrounding a smaller sphere becomes higher, mass transport from the smaller to the larger spheres occurs, via radiation-enhanced diffusion. In this regime, the diameter control with the dose-rate is given by the diffusion process. The deeper fine-dot region is associated with the smaller diffusion due to the less energy deposition. Also, the highest diffusion around the projectile range may be responsible for the depleted zone between the larger spheres and the fine-dot region.

With decreasing the dose rate, the bimodal characteristics diminished, and the particle size became less than 5 nm ϕ at a few μA/cm² [9]. Thus, a wide variation in dose rate enables us to control the diameter of nanospheres, whose depth profile, on average, roughly agrees with the predicted depth profile. Here, it is pointed out that the depth profile actually shifts towards the surface and that the Cu retention in the substrate is dependent on the dose rate. The effect of Cu retention causes variations of optical properties.

By use of the smaller mask of 2 mm ϕ, we succeeded in Cu implantation up to 260 μA/cm², where the limitation was due to loss in Cu retention[10]. The beam-surface interactions play an important role in the mass transport of Cu atoms into the solid.

Figs. 4 and 5 show optical absorbance and reflectance of silica glasses implanted with Cu^- ions to 3.0 x 10^{16} ions/cm² at various dose-rates, using a wider mask of a 12 mm ϕ - aperture. As seen in these figures, absorption and reflection considerably vary with the Cu dose rate, though negative ions alleviate variation more than positive ions[3]. The spectra of absorbance and reflectance vary, not only in the plasmon shape at 2.2 eV but also in

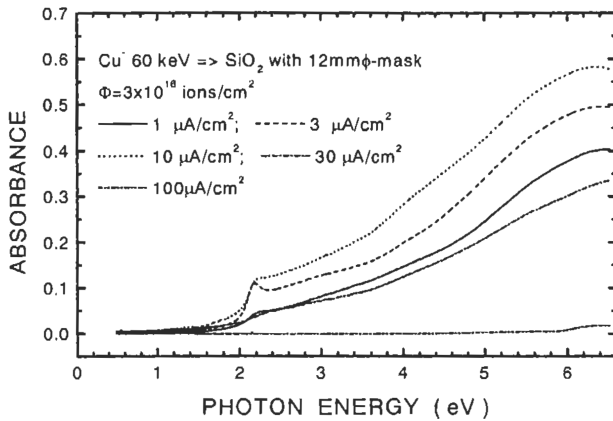

Fig.4 Optical absorbance spectra of silica glasses, 60 keV- Cu^--implanted at various dose rates, with a 12 mm ϕ -mask.

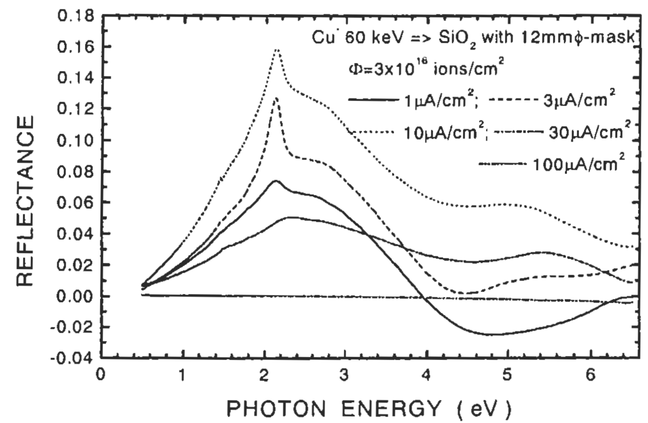

Fig.5 Optical reflectance spectra of silica glasses, 60 keV- Cu^--implanted at various dose rates, with a 12 mm ϕ -mask.

the overall intensity. The former and the latter variations are associated with the nanoparticle morphology and Cu-retention due to beam-surface interactions, respectively. The reflectance shows distinct peaks of the surface plasmon more than the absorbance. Combined analysis of the reflectance and the absorbance allows us to derive the real and imaginary parts of the dielectric constant[11]. There exists an optimum dose rate to promote the surface plasmon peak, i.e., ~3 $\mu A/cm^2$, where the nanospheres dominantly grow, in the case of the 12 mm ϕ -mask.

The bimodal morphology of nanoparticles, which was observed by TEM, seems to cause coexistence of sharp and wide peaks in the absorbance and reflectance spectra.

Fig. 6 shows a dose-rate dependence of absorbance and reflectance around the surface plasmon peak at 2.2 eV. Although intensity of reflectance has a different implication from that of absorption, there is an optimum dose rate around 3-10 $\mu A/cm^2$, for both of them.

Here, comparison with positive ions and with a different mask (boundary condition) is important. A dose-rate dependence of positive Cu ions of 160 keV reported by Magruder III et al [6] was a monotonic and more drastic increase up to 7.5 $\mu A/cm^2$. The divergent variation appears to be moderated by the usage of negative ions. However, the present result indicates that the higher dose-rates may cause a drop of the modification efficiency.

It is pointed out that boundary conditions of a specimen have a significant influence on the dose-rate dependence. Previously, we demonstrated that a 2 mm ϕ -mask enabled us to implant up to 260 $\mu A/cm^2$, but usage of the

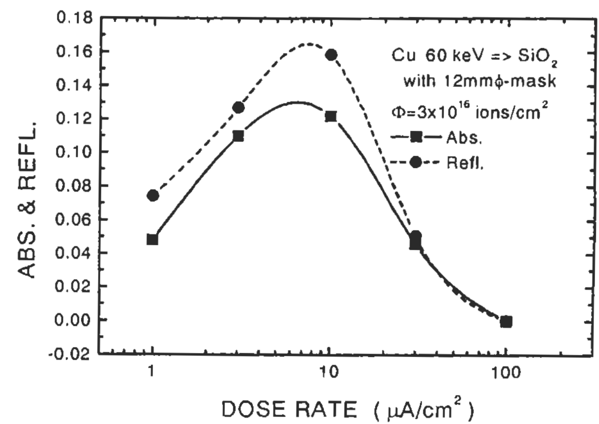

Fig.6 Dose-rate dependence of absorbance and reflectance at the peak around 2.2 eV, for silica glasses Cu^--implanted to 3 x 10^{16} ions/cm^2, using a 12 mm ϕ -mask.

wider mask turned out to reduce the capable dose-rates to less than 100 $\mu A/cm^2$. The difference may be attributed to a change in the effective beam load onto the surface. One of the possible mechanisms of the reduction is surface sputtering which is dependent on the beam load. It was found from an AFM study that surface roughness had a good positive correlation with the dose rate[8]. It may be consistent with the nanoparticle distribution (for instance, see Fig. 3) where the depth profile tends to be shallower than the predicted R_P. Around the optimum dose rate, the nanospheres are fabricated, approximately as predicted by the TRIM code.

Thus, both the outer and inner-solid processes are important in controlling the fabrication kinetics.

As well as the linear optical properties, a nonlinear property of the nanosphere system is

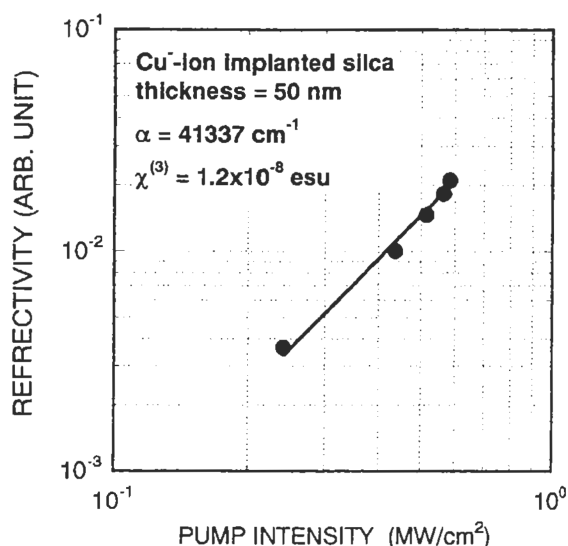

Fig.7 Dependence of reflectivity on pump intensity, for a silica glass implanted with 3 x 10^{16} ion/cm^2. The solid line is a quadratic slope.

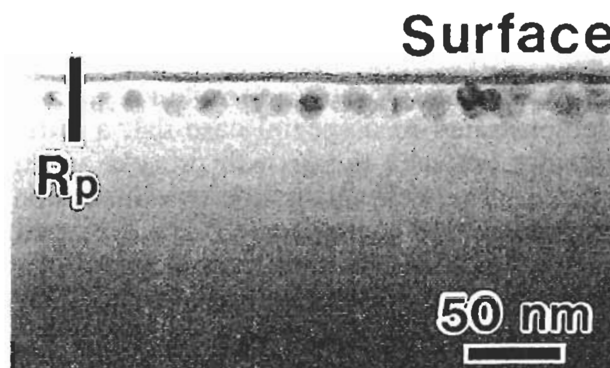

Fig.8 Cross-sectional TEM image of a specimen Cu-implanted at 45 μA/cm^2 with the 12mm ϕ - mask. The R_P i the projectile range of 60 keV-Cu ions.

of concern. Fig. 7 shows pumping-power dependence of nonlinear reflectivity for a Cu implanted silica glass, where the probe intensity was kept constant. As seen in this figure, the nonlinear signal was proportional to the square of pump intensity. It was verified from the result that the signal observed arose from the third-order nonlinearity. For an absorptive medium, reflectivity was corrected with the absorption constant. The $\chi^{(3)}$ -value obtained was 1.2 x 10^{-8} esu, letting L= 50 nm. In comparison to a standard nonlinear substance, CS_2, the bulk signal of the Cu colloids was smaller by three orders of magnitude, but the $\chi^{(3)}$-value normalized by the thickness was 4 orders larger than that of CS_2. This enhancement results from the surface plasmon effect.

The low-energy implantation with high dose-rates was thus carried out and a thin-layered distribution of nanospheres was obtained. Although roundness of the nanoparticles was fulfilled, the depth profile of nanospheres may not be claimed as a 'two dimensional distribution. 'As far as the ion implantation technique is used, some broadening of distribution is inevitable, because of the stochastic collision processes, i.e., the straggling width. The broadening effect remains as a bimodal distribution, even if in-beam precipitation has decreased the broadening of the major particles. This subject should be accepted as a remaining limitation, after the kinetics are controlled.

However, there was a special case where a truly two-dimensional distribution of Cu nanospheres occurred. Fig. 8 shows a cross-sectional TEM image of a specimen, Cu^--implanted at 45 μA/cm^2 with the 12 mm ϕ -mask. This photograph shows a marvelous linear arrangement, i.e., two-dimensional distribution. Also, an interesting feature of Fig. 8 is the apparent absence of the fine-dot zone in the deep region. Another important point is that the average depth of the linear array is much less than the projectile range R_P of the incident ions. It is therefore concluded for this case that a critical balance between the surface recession and the enhanced growth of nanospheres are responsible for the two-dimensional arrangement.

The two-dimensional array of nanospheres is one of the most promising nanostructures for the future applications. Optoelectronic and electric devices, using the nonlinear characteristics, require integration of the thin layers and two-dimensional array, respectively.

4. Conclusions

Fabrication of Cu spherical nanoparticles was carried out by using high-current implantation of negative Cu ions of 60 keV. At the higher dose rates, Cu nanospheres formed near the projectile range and fine dots spread to the deeper range. Nanocrystal growth and the optical properties, i.e., absorption and reflection, were significantly dependent on the Cu dose rate, and were dominated by surface tension and radiation-induced diffusion. It is possible to control the nanoparticle morphology and the optical modification by using kinetic variations.

Negative-ion implantation at 60 keV succeeded in fabricating nanospheres within a narrow layer near the surface. Changing the aperture mask provided another kinetic parameter to control the nanoparticle morphology. It was demonstrated in a special case that a critical balance between the growth process and the sputtering process attains the two-dimensional distribution of nanospheres. The fabrication method provides us with a promising tool for future applications of nanoparticles.

Acknowledgements

The authors are indebted to Nissin High Voltage Co. Ltd. for developing the irradiation facility in collaboration. They are also grateful to Mrs. K. Kono and H. Amekura for collaborating on the facility.

References

1. F. Hache,D. Richard, C. Flytzanis and U. Kreibig, Appl. Phys. A 47 (1988) 347.
2. R. Ruppin, J. Appl. Phys. 59 (1986) 1355.
3. J. Ishikawa, H. Tsuji, Y. Toyota, Y. Gotoh, K. Matsuda, T. Tanjo and S. Sasaki, Nucl. Instrum and Meth. 96 (1995) 7.
4. Y. Mori, A. Takagi, K. Ikegami, A. Ueno and S. Fukumoto, Nucl. Instr. and Meth., B37/38 (1989) 63.
5. J.F. Ziegler, J.P. Biersack and U. Littmark, The Stopping and Range of Ions in Solids, (Pergamon Press, New York, 1985), Chap 8.
6. R.H. Magruder III, R.F. Haglund, Jr, L.Yang, J.E. Wittig and R.A. Zuhr, J. Appl. Phys., 76 (1994) 708.
7. H. Hosono, H. Fukushima,Y. Abe, R.A. Weeks and R.A. Zuhr, J. Non-Cryst. Solids, 143, (1992) 57.
8. N. Kishimoto, V.T. Gritsyna, Y. Takeda, C.G. Lee, N. Umeda and T. Saito, Mater. Res. Soc. Symp. (1998) , in press.
9. N. Kishimoto, V.T. Gritsyna, K. Kono, H. Amekura and T. Saito, Mater. Res. Soc. Symp. Proc. Vol. 438 (1997) 435.
10. N. Kishimoto, V.T. Gritsyna, K. Kono, H. Amekura and T. Saito, Nucl. Instr. and Meth., B127/128 (1997) 579.
11. Y. Takeda, V.T. Gritsyna and N. Kishimoto, unpublished data.